

Shatter cones: (Mis)understood?

Gordon R. Osinski^{1,2*} and Ludovic Ferrière³

2016 © The Authors, some rights reserved; exclusive licensee American Association for the Advancement of Science. Distributed under a Creative Commons Attribution NonCommercial License 4.0 (CC BY-NC). 10.1126/sciadv.1600616

Meteorite impact craters are one of the most common geological features in the solar system. An impact event is a near-instantaneous process that releases a huge amount of energy over a very small region on a planetary surface. This results in characteristic changes in the target rocks, from vaporization and melting to solid-state effects, such as fracturing and shock metamorphism. Shatter cones are distinctive striated conical fractures that are considered unequivocal evidence of impact events. They are one of the most used and trusted shock-metamorphic effects for the recognition of meteorite impact structures. Despite this, there is still considerable debate regarding their formation. We show that shatter cones are present in several stratigraphic settings within and around impact structures. Together with the occurrence of complete and “double” cones, our observations are most consistent with shatter cone formation due to tensional stresses generated by scattering of the shock wave due to heterogeneities in the rock. On the basis of field mapping, we derive the relationship $D_{sc} = 0.4 D_a$, where D_{sc} is the maximum spatial extent of in situ shatter cones, and D_a is the apparent crater diameter. This provides an important, new, more accurate method to estimate the apparent diameter of eroded complex craters on Earth. We have reestimated the diameter of eight well-known impact craters as part of this study. Finally, we suggest that shatter cones may reduce the strength of the target, thus aiding crater collapse, and that their distribution in central uplifts also records the obliquity of impact.

INTRODUCTION

Impact cratering is, arguably, the most important and fundamental geological process in the solar system (1, 2). Impact craters are one of the most common geological landforms on the majority of rocky terrestrial planets, asteroids, and many of the rocky and icy moons of the inner and outer solar system. It is also now apparent that impact events have profoundly affected the origin and evolution of Earth and produced benefits in the form of economic mineral and hydrocarbon deposits (3). The destructive geological, environmental, and biological effects of meteorite impact events are well known. This is largely due to the discovery of the ~180-km-diameter Chicxulub impact structure, Mexico, and its link to the mass extinction event that marks the end of the Cretaceous period ~66 million years ago (4). In recent years, it has also become apparent that, once formed, impact events also have certain beneficial effects, particularly for microbial life (5, 6). This may have important implications for our understanding of the origin and evolution of early life on Earth, and possibly other planets, such as Mars.

The study of impact processes and products is a multidisciplinary endeavor, synthesizing observations from the field, laboratory, and spacecraft, together with results of experiments and numerical modeling. However, impact craters on Earth provide the fundamental and unique opportunity to ground-truth the products of impact events. To date, approximately 190 impact craters have been recognized on Earth. Early discoveries of impact craters on Earth relied on the presence of meteoritic fragments around topographic depressions (7). However, this method resulted in the identification of only a handful of structures. This all changed in the 1960s with the recognition of shock-metamorphic effects in rocks and minerals (8). Shatter cones are one of the first proposed shock-metamorphic effects (9) and the only one that is visible

at the hand specimen and outcrop scale (10). First recognized at the Steinheim impact structure, Germany (11), shatter cones consist of striated conical to curvilinear fractures that typically occur in hierarchical networks (Fig. 1A). They have only been recognized in meteorite impact craters and their ejecta deposits (12), meteorites (13), and nuclear (14) and large-scale conventional (15) explosion craters. Shatter cones start to form at pressures as low as ~2 GPa (12), much lower than any other unequivocal shock-metamorphic features [for example, planar deformation features (PDFs) in quartz form at >8 to 10 GPa], which means they form in large volumes of target rock extending further away from the point of impact than any other shock effect. Because of these properties, shatter cones remain the most useful criterion for the recognition of new meteorite impact structures, particularly deeply eroded ones, where they often represent the only observed shock-metamorphic effect [for example, Île Rouleau (16), Presqu'île (17), and Tunnunik (18) in Canada].

Despite their widespread occurrence and importance in confirming meteorite impact craters, the origin of shatter cones remains poorly understood and actively debated, with various formation mechanisms having been proposed over the past 50 years (19–23). This is perhaps not surprising given the contradictory observations and various misconceptions that pervade the literature. Several fundamental properties of shatter cones remain ambiguous. For example, most reports of shatter cones are from the central uplifts of complex craters, although some workers have suggested that they form in the rims of complex impact craters (24), with fragments of shatter cones in impact breccias being rare (25). Estimates for the timing of shatter cone formation ranges from the contact and compression [for example, (21)] to the modification stage of crater formation [for example, (26)]. Finally, even the use of the word “cone” has been called into question, with some authors suggesting that shatter cones are not conical (19).

Here, we provide new observations of shatter cones from several complex impact craters in various target rocks and in different preservation states (Table 1). Together, these observations provide new insights into the formation of shatter cones, their spatial distribution and

¹Centre for Planetary Science and Exploration, University of Western Ontario, 1151 Richmond Street, London, Ontario N6A 5B7, Canada. ²Department of Earth Sciences and Department of Physics and Astronomy, University of Western Ontario, London, Ontario N6A 5B7, Canada. ³Natural History Museum, Burgring 7, A-1010 Vienna, Austria. *Corresponding author. Email: gosinski@uwo.ca

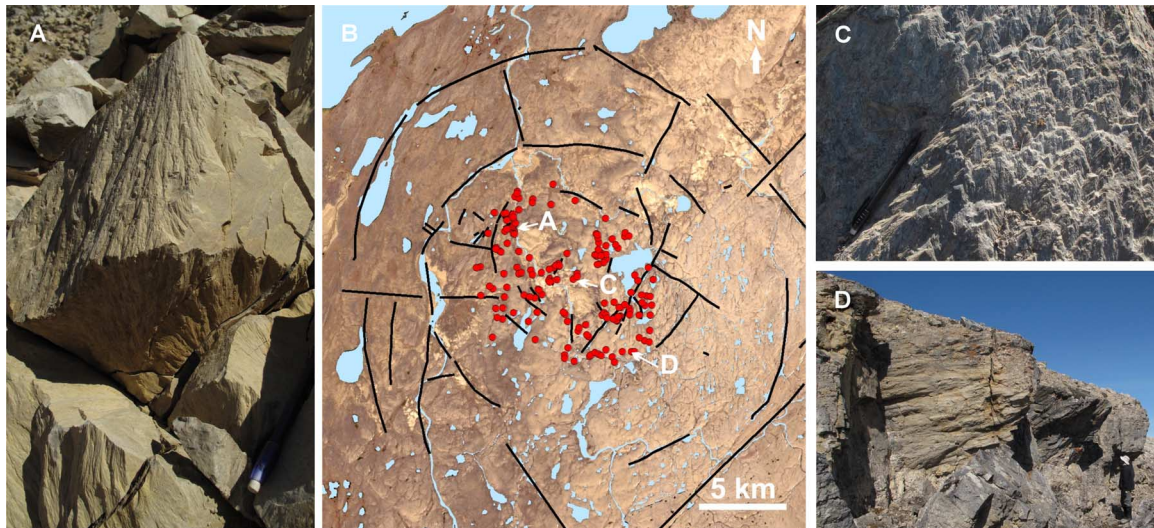


Fig. 1. Shatter cone morphologies and distribution at the Tunnunik impact structure (Northwest Territories, Canada). (A) Shatter cones in dolomite (14-cm-long pencil for scale). (B) Map of shatter cone distribution (red dots) superposed on a Landsat 8 image. Black lines indicate major faults. Locations of images in (A), (C), and (D) are shown. (C) Shatter cones in dolomite from the center of the structure (14-cm-long pencil for scale). (D) Shatter cones in dolomite from the outer edge of the central uplift (person for scale).

Table 1. Important attributes of the studied sites and stratigraphic and lithologic setting of shatter cones. These observations are the result of fieldwork conducted for this study. In many instances, shatter cones have previously been recorded at these structures and references have been provided where appropriate. S, sedimentary; C, crystalline; M, mixed target of sedimentary rocks overlying crystalline basement; CU, central uplift; CFill, crater fill; X, present; np, not preserved (that is, the setting is not preserved or exposed); ?, unknown (that is, the setting is preserved and exposed, but it is unknown whether shatter cones are present); b, bedrock, lb, lithic impact breccia; mb, impact melt-bearing breccia; mr, impact melt rock.

Name	D_a^*	Target	Erosional level [†]	Stratigraphic and lithologic setting in crater			
				CU	Dikes	CFill	Ejecta
Haughton	23	S	2	Xb [cf., (64)]	Xlb,mr	Xmr	Xlb,mr
Mistastin	28	C	2	Xb [cf., (66)]	?	np	Xlb,mb
Ries	26	M	2	Xb [cf., (65)]	Xmb	X	X [cf., (40, 65)]
Sierra Madera	20	S	6	Xb [cf., (30)]	Xlb [cf., (30)]	np	np
Slate Islands	30	C	6	Xb [cf., (32)]	Xlb [cf., (32)]	np	np
Tunnunik	28	S	6	Xb [cf., (18)]	Xlb	np	np
West Clearwater	36	C	4	Xb [cf., (67)]	Xmr	Xlb,mb,mr	np

*Apparent crater diameter. For Sierra Madera, we have updated the diameter on the basis of this study (see Table 2). [†]Erosional level: 1, ejecta largely preserved; 2, ejecta partly preserved, rim partly preserved; 3, ejecta eroded, rim partly preserved; 4, rim largely eroded, crater-fill breccias/melt rocks preserved; 5, crater-fill breccias/melt rocks partly preserved; 6, crater-fill breccias/melt rocks eroded, isolated breccia dikes; 7, eroded below crater floor.

stratigraphic setting within impact craters, and their potential role in weakening the target before crater collapse.

RESULTS

Spatial distribution of shatter cones

The spatial distribution of shatter cones is known for only a handful of impact structures [for example, Charlevoix (27), Keurusselkä (28), Rochechouart (29), Sierra Madera (30), Siljan (31), Slate Islands (32),

Sudbury (33), and Vredefort (24)]; however, it is noteworthy that all of these structures are either poorly exposed, deeply eroded, deformed, or all of the above. Hence, there is considerable ambiguity as to whether the extent of shatter cones has been accurately mapped and, when it has, how this relates to the original crater diameter. We have performed detailed mapping of the newly discovered Tunnunik impact structure, Northwest Territories, Canada (18), and further mapping of the Haughton impact structure, Nunavut, Canada (34). Both of these structures are exceptionally well exposed and offer two different erosional levels (Table 1). Furthermore, they both formed in thick sequences of sedimentary rocks

of the Arctic Platform overlying crystalline metamorphic rocks of the Precambrian Canadian Shield. Figure 1B shows the distribution of shatter cones at the Tunnunik structure. In many instances, we could trace the nonoccurrence of shatter cones to distances of <100 m and in outcrops of the same lithology. We could also map the outermost concentric normal faults (Fig. 1B), which define the apparent crater diameter (D_a) (35) at 28 km. Shatter cones are distributed over an area of 10.1 km × 12.0 km. Thus, the maximum spatial extent of shatter cones is $D_{sc} = 0.36$ to $0.43 D_a$.

It is noted that the distribution of shatter cones at Tunnunik is distinctly elliptical. The simplest explanation, which agrees with theory (2), is that this is the result of an oblique impact. Although there is a fault with post-impact movement that transects the Tunnunik structure (Fig. 1B), our field studies show that this is a steep normal fault with virtually no horizontal displacement and only minor rotation of the southern block. Hence, this fault has slightly changed the orientation of shatter cones in the southern block, but has not affected their distribution, which is consistent with no offset whatsoever of the shatter cones across this fault. To our knowledge, this is the first time that a noncircular “primary” distribution of shock effects has been recorded in a natural setting that is not notably affected by tectonic overprint. Thus, shatter cone distribution provides an important new method to gauge the obliquity of impact. Other proxies to determine obliquity, such as the pattern of the ejecta deposits (36), are only viable techniques in planetary craters that preserve these deposits.

The Haughton impact structure is a much less eroded impact structure than Tunnunik, with a well-constrained apparent crater diameter of 23 ± 0.5 km (37). Exposure is excellent along the Haughton River valley that transects the outer edge of the central uplift. Shatter cones were mapped out to a radial distance of up to 4.5 km along this valley, such that $D_{sc} = 0.39 D_a$. Given the fact that this represents the median of the range $D_{sc} = 0.36$ to $0.43 D_a$ determined for the elliptical distribution at Tunnunik, we propose that the relationship $D_{sc} = 0.4 D_a$ should be applicable for all midsize complex impact craters on Earth, with some caveats that will be discussed later.

The relationship of shatter cone distribution to apparent crater diameter has substantial implications to estimate the size of eroded impact structures on Earth, which represents the majority of the exposed (that is, nonburied) complex structures. In most of these cases, neither the crater rim nor the diameter of the central uplift is well known or known at all. It is outside the scope of this contribution to reestimate the size of all craters on Earth, but we provide new estimates for the apparent crater diameter of the Charlevoix (70 km), Gosses Bluff (32 km), Keurusselkä (36 km), Luizi (15 km), Presqu'île (15 km), Rochechouart (32 km), Sierra Madera (20 km), and Siljan (75 km) impact structures in Table 2. Our new, more accurate method substantially changes the diameter of some of these craters, which has important implications for recent studies that have used the crater size frequency of terrestrial impact structures to make inferences on the impact flux (38, 39).

Stratigraphic and lithologic setting of shatter cones

Previous models of formation of shatter cones, and most previous studies of shatter cones, have been conducted on deeply eroded impact craters, where they are typically only found in situ in the eroded central uplift [for example, Sierra Madera (30), Kentland (19), and Vredefort (24)]. It is a widely held view that shatter cones predominantly occur in rocks of the central uplift. However, it is important to consider that the rocks of the central uplift are invariably the last rocks to be eroded away in an impact

crater, which, we suggest, has resulted in an observational bias. We have carried out fieldwork at seven midsize impact structures (Table 1) ranging from 20 to 36 km in diameter. Although shatter cones occur in the central uplifts of all of these structures (for example, Figs. 1 and 2, A and B, and Table 1) as has been previously reported (see references in Table 1), we draw attention to several other important stratigraphic settings (Fig. 2). In the three studied structures with preserved proximal ejecta, shatter cone clasts occur in impactites ranging from lithic impact breccias to clast-rich impact melt rocks (Table 1 and Fig. 2, A to C). Shatter cone clasts have also been reported in distal ejecta from the Ries impact structure (40).

We have observed breccia dikes intruded into the crater floor and containing shatter cone clasts in six of seven studied structures (Table 1 and Fig. 2, A and D). Finally, at the Haughton and West Clearwater structures, where the crater-fill deposits are very well preserved, we have observed abundant shatter cone clasts in a range of impactite types (Table 1 and Fig. 2, A and E). Shatter cone clasts have been reported in isolated exposures of lithic and impact melt-bearing breccias at the heavily eroded Gosses Bluff (41) and Vista Alegre (42) impact structures, which most likely represent crater-fill deposits rather than breccia dikes.

In both the Haughton and Tunnunik structures, the nonoccurrence of shatter cones occurs at ~1 to 2 km inside the outer edge of uplifted strata. There are no shatter cones in the crater rim region, which is something that was previously suggested by Wieland *et al.* (24) to occur at the Gosses Bluff, Sierra Madera, and Vredefort impact structures. However, at Gosses Bluff, the distribution of shatter cones has been mapped in detail with the maximum extent of shatter cones cited as ~13 km and a previous apparent crater diameter of ~24 km (41). At Sierra Madera, shatter cones are mapped over a region of ~8 km in diameter (30), which we confirmed in this study. Even with the previous apparent crater diameter of 13 km, shatter cones do not occur in the rim region of Sierra Madera. As proposed in the previous section and presented in Table 2, we suggest that both Gosses Bluff and Sierra Madera are larger than previously expected. We thus propose that shatter cones are only found in situ in central uplifts.

In terms of allochthonous impactites, our field observations, together with a reappraisal of previous studies, demonstrate that shatter cone clasts are present and often abundant in all major stratigraphic settings within impact craters and in all classes of impactites (lithic impact breccias, impact melt-bearing breccias, and impact melt rocks) (Fig. 2).

Orientation and morphology of shatter cones

Much has been made of the orientation and morphology of shatter cones in the literature. It is frequently stated that shatter cone apices are typically “oriented in one direction” and that “cone axes are generally parallel” (10). These properties have frequently been used to determine the center of deeply eroded impact structures [for example, Rochechouart (29)]. However, at both the Tunnunik and Haughton impact structures, shatter cones with apices pointing in variable—and often completely opposite—directions are the norm, not the exception (Figs. 1A and 3, A to C). Observations of apices pointing both up and down were also made at the Vredefort structure (24). In terms of morphology, recent studies concluded that shatter cones are “not separable, isolated objects within the rock mass” and that “complete cones are very rare” (19). Our observations of shatter cones at the Haughton and Tunnunik impact structures also clearly contradict this view (Figs. 1A and 3A). We have also observed shatter cones with very curved nonplanar surfaces (Fig. 3D).

We documented a gradual but distinct change in shatter cone morphology and size with increasing radial distance from the center of the

Table 2. New estimates for the apparent crater diameter of selected complex impact structures.

Name	D (EID)*	D (literature) [†]	Target	Erosion level [‡]	D_a (this study) [§]	Notes
Charlevoix	52	28–52	M	6	70	Initial studies yielded estimates in the order of ~30 km (68, 69). Later studies have generally put the diameter at ~52 km, which corresponds to a ring of outer hills (70, 71). The outer limit of shatter cones has been mapped at 14-km radius from the crater center (27). On the basis of this mapping and using $D_{sc} = 0.4 D_a$, we estimate a minimum apparent crater diameter of this structure at 70 km.
Gosses Bluff	24	24	S	6	32	The diameter of Gosses Bluff is typically assumed to be a subtle topographic circular feature at ~24-km diameter (41). Exposure is virtually zero in this region. Shatter cones have been accurately mapped in the well-exposed circular ring of hills known as Gosses Bluff out to a radius of 6.5 km. On the basis of this detailed mapping and using $D_{sc} = 0.4 D_a$, the apparent crater diameter of this structure is estimated fairly robustly at 32 km.
Keurusselkä	30	10–30	C	6	36	The Keurusselkä impact structure is a heavily eroded structure in central Finland that was first recognized by the presence of shatter cones (72). There is no obvious topographic form, and estimates of the original crater diameter range from 10 to 30 km (28, 72–74). However, detailed mapping has shown that shatter cones are present over an area of 14 km across (73). On the basis of this detailed mapping and using $D_{sc} = 0.4 D_a$, the apparent crater diameter of this structure is estimated fairly robustly at 36 km.
Luizi	17	17	S	5/6	15	The diameter of the Luizi impact structure was estimated to be about 17 km (75) using a combination of satellite images and a digital elevation model. Ferrière <i>et al.</i> (75) reported that shatter cones are restricted only to the inner 3.2 km of the structure. However, during a second field campaign that included more comprehensive mapping, shatter cones were mapped over a region of ~6-km diameter in the center of the structure [this study; (76)]. Using $D_{sc} = 0.4 D_a$, we can estimate the apparent crater diameter of this structure at 15 km.
Presqu'île	24	12–24	C	6/7	15	Little previous work has been done on this structure. Higgins and Tait (17) provided size estimates ranging from 12 to 24 km in diameter. Shatter cones have been mapped over an area defined by a circle with a 6-km diameter (17). Using $D_{sc} = 0.4 D_a$, we can estimate a minimum apparent crater diameter of this structure at 15 km. However, further fieldwork with detailed mapping is required to better determine the distribution of shatter cones.
Rochechouart	23	15–50	C	5	32	A wide range of estimates have been suggested for the Rochechouart impact structure. Initially, a “minimum diameter” of 15 km was proposed (77). Studies in the 1970s proposed diameters in the range of 18 to 25 km (78) and 20 to 25 km (29). Estimates up to 40 to 50 km have also recently been proposed (79). Shatter cones have been mapped over an area defined by a circle with ~12- to 14-km diameter (29). This yields an estimate for the apparent crater diameter of this structure at 32 km.
Sierra Madera	13	13–16	S	6	20	The widely cited diameter of 13 km comes from early mapping efforts and corresponds to the “outer limit of deformation” (30). However, it is notable that there is virtually no exposure beyond the area mapped by Wilshire <i>et al.</i> (30). Goldin <i>et al.</i> (80) conducted numerical modeling studies with rim (final crater) diameters (D) of 12 and 16 km. These authors conclude that “models of the 16-km-diameter crater better reproduce the crater geometry, but fail to agree with previous workers’ interpretations and observations of the extent and degree of deformation.” On the basis of the mapping by Wilshire <i>et al.</i> (30), $D_{sc} = 8$ km, which results in an apparent crater diameter of 20 km according to our relationship for D_{sc} . Given $D < D_a$ (35), this is in keeping with the numerical modeling studies of Goldin <i>et al.</i> (80).
Siljan	52	52–65	M	6	75	A diameter of 52 km is frequently cited on the basis of the work by Grieve (81). The most recent estimates based on the limit of “intense fracturing” is 65 km (82), although these authors also state that the diameter could still be larger. Recently, Holm <i>et al.</i> (31) conducted the most comprehensive study of shock metamorphism at Siljan to date. They describe shatter cones extending to a radius of between 15 and 16 km from the crater center. On the basis of this detailed mapping and using $D_{sc} = 0.4 D_a$, we can estimate a minimum apparent crater diameter of this structure fairly robustly at 75 km.

*Diameter given in the Earth Impact Database (EID) (www.passc.net/EarthImpactDatabase/index.html). Note that no distinction is made in this database between rim (final crater) diameter and apparent crater diameter. [†]Estimates from the literature. Note that typically no distinction is made between rim (final crater) diameter and apparent crater diameter. [‡]Erosion level: 1, ejecta largely preserved; 2, ejecta partly preserved, rim partly preserved; 3, ejecta eroded, rim partly preserved; 4, rim largely eroded, crater-fill breccias/melt rocks preserved; 5, crater-fill breccias/melt rocks partly preserved; 6, crater-fill breccias/melt rocks eroded, isolated breccia dikes; 7, eroded below crater floor. [§]Apparent crater diameter calculated based on our relationship for shatter cones, $0.4 D_a$. Given most of the craters in this table are very eroded, this should be taken as a minimum apparent crater diameter.

Tunnunik impact structure. At the crater center, coning is pervasive and cones are generally a few centimeters in size (Fig. 1C). The amount of coning decreases outward such that, for much of their distribution, cones are well defined and range from a centimeter to decimeter in size (Fig. 1A). Finally, at the outer edge of their range, shatter cones are fewer in number and isolated, are more poorly defined, and reach their maximum size of ten >1 m in length (Fig. 1D). Although the exposure is poorer at Haughton and the Slate Islands, we see the same pattern [cf., earlier workers who report the most extreme coning in the center of the Slate Islands (32) and with large, more isolated, meter-sized cones occurring near their outer limit (43)]. It is interesting to note that at Charlevoix, the best developed shatter cones occur in an annulus at ~7-km radius with a “decrease in quality of development inward and outward from this zone” and with the largest examples occurring near the outer spatial extent (44).

DISCUSSION

Using shatter cones to estimate crater size

One of the first and most important questions asked about any impact crater is “how big is it?” For craters on other planetary bodies where recent or ongoing plate tectonics, volcanism, and active erosional processes are lacking, determining crater size is relatively straightforward and is achieved by measuring the diameter of the topographically high crater rim (35). On Earth, erosion and other geological processes have either destroyed or obscured the topographic rim at the vast majority of

impact craters. Thus, other methods to determine the size of a crater are required. For the majority of the impact structures on Earth, the apparent crater diameter (D_a) is the only measurable diameter and is defined as “the diameter of the outermost ring of (semi-) continuous concentric normal faults” (Fig. 2A) (35). Unfortunately, in the majority of the terrestrial craters, there is too little exposure to allow detailed mapping to be conducted, the structures are buried and lack detailed seismic studies, or there have simply not been any detailed field studies performed.

Because of these limitations, previous workers have turned to using the spatial distribution of various impact phenomena (for example, shatter cones, PDFs in quartz, impact breccia dikes, and diameter of the melt sheet) to estimate crater size. Several studies have used the suggestion that the limit of shatter cones is $\leq D_{tc}$ (transient cavity diameter) [for example, Grieve *et al.* (45) and Therriault *et al.* (46)]. This provides only a very crude estimate, and furthermore, determining the diameter of the transient cavity for most craters is extremely difficult, or impossible, because it is destroyed during the modification stage of complex crater formation (2). In a related study, the diameter of the zone of shatter cones for the Carswell, Ries, and Rochechouart impact structures was reported to be 0.80, >0.5, and 0.59 D_{tc} , respectively (47), although no observational data were provided on which to gauge these values. The only other previous study to attempt to relate shatter cone distribution to apparent crater diameter is the work of Lakomy (48), which was only reported in a non-peer-reviewed conference abstract. This author provides a plot of the maximum radial extent of various shock features versus apparent crater diameter. Neither the data on which the

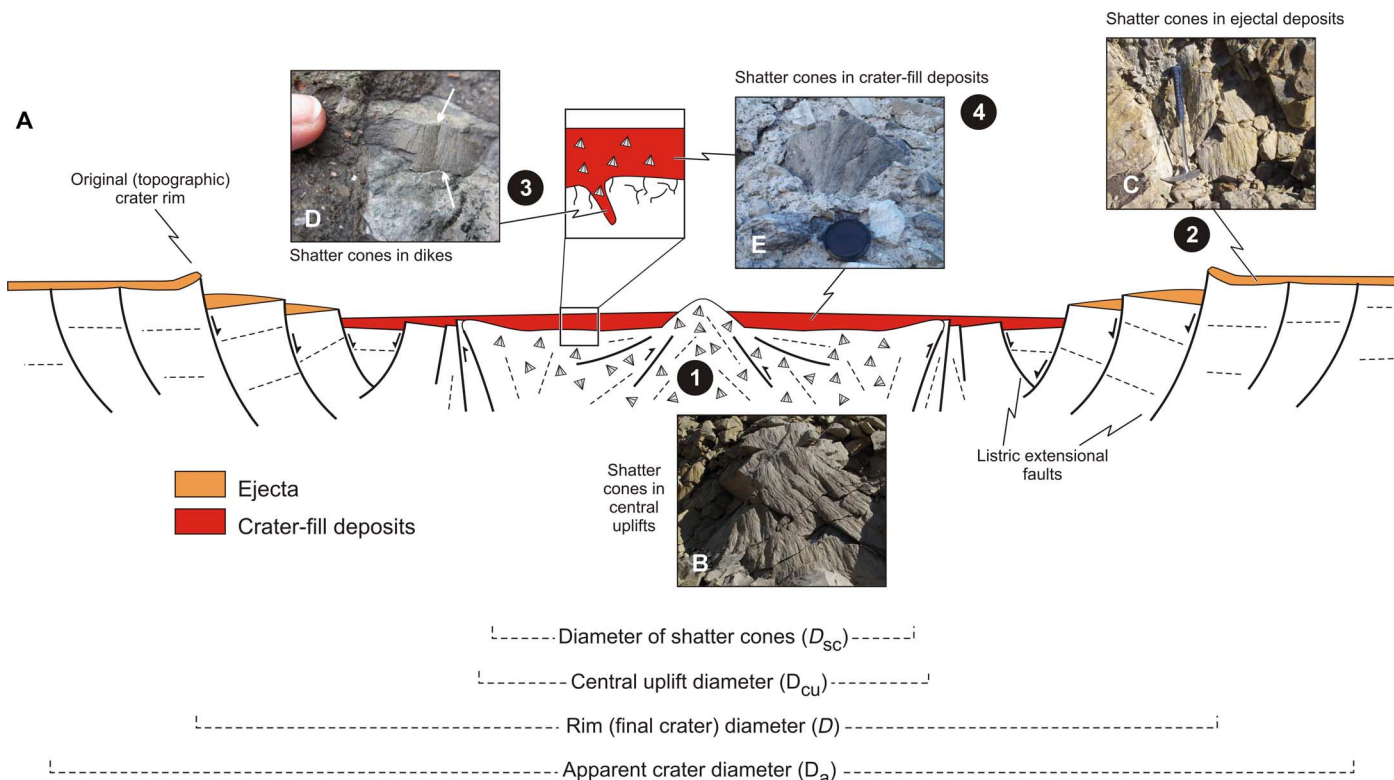


Fig. 2. Stratigraphic settings of shatter cones in complex impact craters. (A) Schematic cross section of a typical complex impact crater in the size range ~10 to 150 km in diameter. (B) Shatter cones in the central uplift of the Tunnunik impact structure (15-cm-long pen for scale). (C) Shatter cones in ejecta from the Haughton structure (35-cm-long rock hammer for scale). (D) Shatter cone clast (arrows) in a breccia dike from the Slate Islands structure (15-cm-long pen for scale). (E) Shatter cone clast in the crater-fill impact melt rock at the Haughton structure (7-cm-diameter lens cap for scale).

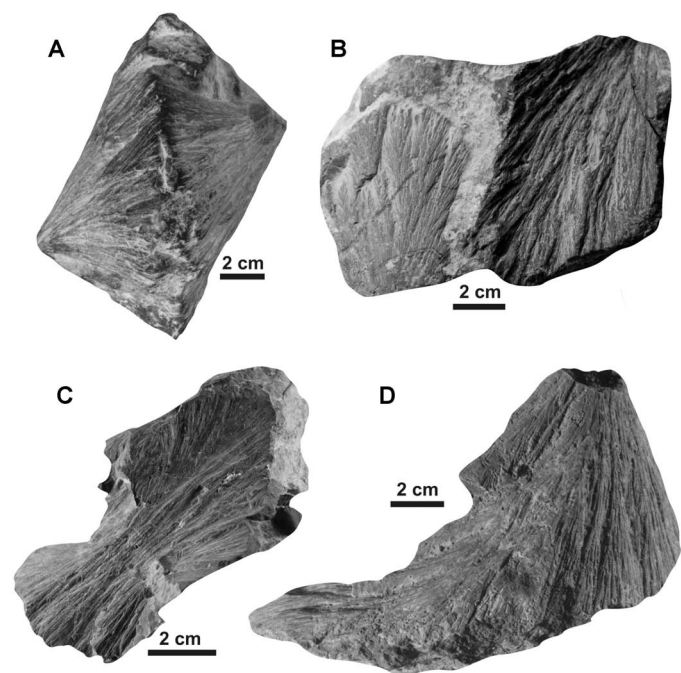


Fig. 3. Shatter cone morphologies. (A to D) Hand specimen images of shatter cones from the Haughton impact structure.

plot is based nor the references from which the data were obtained are provided; however, most craters yield estimates of $\sim D_{sc} = 0.5$ to $0.6 D_a$.

One of the major results of our fieldwork at the Haughton and Tunnunik impact structures is the determination of the relationship $D_{sc} = 0.4 D_a$. We suggest that this relationship represents a substantial improvement over previous estimates for the following two fundamental reasons. First, the apparent crater diameter (D_a) for both the Haughton and Tunnunik structures has been determined to be better than ± 1 km. Second, the disappearance of shatter cones that delineates the diameter of the zone of shatter cones (D_{sc}) has been determined to be better than ± 1 km. We suggest that this is the main reason for the discrepancy between our estimate for D_{sc} and that of previous studies (47, 48). It is also important to note that the rim (final crater) diameter (D) (35) (Fig. 2A), which is calculated in numerical models and measured in pristine planetary craters, is typically not known for terrestrial craters and is not the same as D_a [$D < D_a$ (35)]. However, it has been constrained from field mapping at 16 km for Haughton (37), which results in the relationship $D_{sc} = 0.55 D_a$.

How applicable is the relationship $D_{sc} = 0.4 D_a$ to other craters? It is important to note that the relationship $D_{sc} = 0.4 D_a$ is only applicable for shatter cones that are unequivocally in situ within the central uplift. Thus, with a few caveats and on the basis of the following discussion, we suggest that this relationship is applicable for all complex impact craters on Earth in the range of >2 km to ~ 150 km in diameter. We suggest these limits because craters in this size range typically display similar attributes [that is, a central core of uplifted rocks, a surrounding relatively flat crater floor, and a faulted rim zone (49)]. Smaller craters will be either simple or so-called transitional craters, in which the spatial extent of shatter cones may be different because of less collapse during the modification stage. At diameters above ~ 150 to 200 km on Earth, the central uplifted core or central peak is replaced with a peak ring, as in the case of the 180-km-diameter Chicxulub impact structure, Mexico (50). Although the origin of peak rings is still debated, it seems likely that the outward collapse of

an original central peak occurs (51), which would obviously completely alter the distribution of shock effects, including shatter cones.

In terms of erosion level, we are confident that the relationship holds for a wide range of erosion levels given the similarity in D_{sc} between Haughton [erosion <200 m (34)] and Tunnunik [erosion >1 km (18)]. A further consideration is target lithology. It is well known that the composition and physical properties of the target rocks affect many aspects of the impact cratering process. Although the effect on impact melting and impactites is relatively well understood (52, 53), the physics of rock failure and deformation during crater collapse is not (54). Of relevance to this discussion is the comparative numerical modeling (55) and field and laboratory (53) study of midsize impact craters in crystalline versus sedimentary targets, which considered the similarly sized Haughton, Ries, Mistastin, and El'gygytyn impact structures. These studies showed that the distribution of shock pressures is not significantly different in sedimentary or crystalline rocks [for example, Fig. 3 in Osinski *et al.* (53) shows that the 2-GPa shock isobar is at approximately the same radial distance ± 1 km in the Haughton, Ries, and El'gygytyn models]. However, porosity in the target rocks was not considered in these models. In a study of impact melt production, Wünnemann *et al.* (56) showed that the shock wave decays faster in more porous materials, which would decrease the radial extent of shock isobars and, therefore, also reduce D_{sc} in more porous targets. However, this is effectively cancelled out by the fact that porosity reduces the shock pressures required for melting (56). The lowering of the threshold for melting in more porous targets is mirrored in certain shock-metamorphic effects. For example, diaplectic glass forms at pressures as low as 5.5 GPa in sedimentary rocks (57), whereas it forms at a pressure of ~ 32.5 GPa in crystalline rocks (58). Unfortunately, to our knowledge, experiments or models looking at shatter formation in porous versus nonporous targets have not been carried out to date.

Thus, although we cannot rule out a different value of D_{sc} in different target lithologies, we suggest that it should still be $\sim 0.4 D_a$. It is worth noting that it is well known that porosity decreases with depth in Earth's crust so that if there is an effect, it will be more significant in small complex impact craters that only penetrate the uppermost crust where porosity is more variable. Finally, there are well-documented differences in crater morphology and products from impacts into unconsolidated and/or saturated marine impact craters (59), such that it is even unclear as to whether shatter cones even form in such scenarios.

The origin of shatter cones

Here, we use our new field observations together with previous models for shatter cone formation. Johnson and Talbot (21) first suggested that shatter cones form when the elastic precursor of the shock front is scattered by a heterogeneity in the rock, whereas others suggested that shatter cones are tensile fractures formed due to interference between the incident shock waves and reflected stress waves (22). More recently, Sagy *et al.* (19, 20) proposed that shatter cones are dynamic fractures produced by nonlinear front waves that propagate along a fracture front. In this model, shatter cones are not actually cones but rather spoon-like branched fracture surfaces. This model clearly cannot explain our observation of complete cones and cones with apices pointing in opposite directions, including spectacular double cones (Figs. 1A and 2D).

In another model, Baratoux and Melosh (23) built upon earlier suggestions (21) invoking heterogeneities in rocks as initiation points for shatter cone formation. However, in contrast to the earlier model, this new model proposes that the interference of a scattered elastic wave by

heterogeneities results in a tensional hoop stress occurring during the decay—and not buildup—of the shock wave, which produces conical fractures. Our observations are broadly consistent with this model. The presence of shatter cones in ejecta, crater-fill deposits, and dikes clearly demonstrates that they must form after the passage of the shock front but before the passage of the rarefaction wave that initiates the excavation flow. This is consistent with reports of shatter cone surfaces in meteorites (13) and argues against shatter cones forming “relatively late in the formation” of craters (26).

However, to also account for the widespread occurrences of cones pointing in several different directions, we propose that as the shock front expands, it is reflected and refracted due to impedance contrasts in the target. In sedimentary targets, such as at Houghton and Tunnunik, sedimentary layering is proposed to be the primary control. This is consistent with the report of shatter cones forming at, and oriented around, concretion-host claystone interfaces from the Steinheim impact structure (60). Preexisting joints and faults in any target would also result in the same situation. This can account for the close spatial association of shatter cones and joint surfaces as observed at the Keurusselkä structure (28).

It is suggested that the change in shatter cone morphology—from pervasive small cones in the crater center to large, more discrete cones at their farthest extent—is due to the increasing width of the shock front as it radiates outward, as predicted from the theory (2), but not considered in previous shatter cone formation models. The theory also suggests that as the shock front radiates outward, it is not just one discrete front but rather a series of multiple fronts (2), which would allow further reflection(s) and interference(s), resulting in the different morphologies that are seen in the field (Figs. 1 and 2).

Implications for complex crater formation

An important finding from our fieldwork is that when exposure is excellent, such as at the Tunnunik and Houghton structures in the Canadian Arctic, we observe that shatter cones are abundant (for example, Figs. 1 and 2, A and C to G). At Houghton and Tunnunik, we documented shatter cones in >90% of the outcrops we visited in the central uplift. At Houghton, we counted shatter cone surfaces on clasts in the crater-fill deposits and found them on ~50 to 60% of the clasts. Therefore, an important conclusion is that, following the passage of the shock wave, the target rocks in the interior of the crater are pervaded by shatter cones. Furthermore, as demonstrated by the fact that shatter cone clasts occur in impact breccias (Fig. 2) and that target rocks in central uplifts break along shatter cone surfaces (Fig. 1, A, C, and D), it appears obvious that shatter cones represent planes of weakness in rock.

Given these observations, we hypothesize that the formation of shatter cones may aid in weakening the target rocks, which is deemed necessary for crater collapse to occur but for which there remains no single widely accepted model (2). Thus, in addition to the well-known potential weakening mechanisms of acoustic fluidization (61) and lubrication of faults by melt (62), we suggest that future modeling efforts should investigate the potential for the presence of shatter cones to also aid in weakening the target rocks in complex impact craters. Many numerical models now include damage as a parameter, where it provides a measure of the degree of fracturing (63). Collins *et al.* (63) note that “although numerical models predict that much of the target becomes ‘damaged’ during the cratering process, the target rock within this zone will likely reflect a range of deformation features.” These authors do not discuss shatter cones in the context of their numerical models, but perhaps, shatter cones are a physical manifestation of the damage caused by shear failure driven

by the passage of the shock wave in their simulations. Future collaborative efforts to accurately compare model results of deformation with field measurements of strain are warranted.

MATERIALS AND METHODS

Here, the observations presented are the outcome of several months’ cumulative fieldwork at the impact structures listed in Table 1. Fieldwork was conducted at the Houghton impact structure over several summers (1999–2010, 2013) at the Ries impact structure in September 2000, April 2001, September 2005, and June 2010; at the Mistastin Lake impact structure in September 2009; at the Sierra Madera impact structure in March 2004 and 2006; at the Tunnunik impact structure in July 2012 and July to August 2015; and at the West Clearwater Lake impact structure in August to September 2014. Observations from the Slate Islands impact structure came from G.R.O.’s research team, which carried out fieldwork in August 2013 and July 2014. Additional field data from the Mistastin Lake impact structure from field expeditions in September 2010 and 2011 came from G.R.O.’s research team. In addition to the structures listed in Table 1, G.R.O. and L.F. had conducted studies of shatter cones at the Charlevoix, Crooked Creek, Decaturville, Gosses Bluff, Luizi, and Rochechouart impact structures, which further informed this study. Fieldwork was augmented by a detailed literature review of shatter cone occurrences in approximately 150 of the 188 or so confirmed impact structures on Earth.

REFERENCES AND NOTES

1. G. R. Osinski, E. Pierazzo, Eds., *Impact Cratering: Processes and Products* (Wiley-Blackwell, Oxford, 2012).
2. H. J. Melosh, *Impact Cratering: A Geologic Process* (Oxford Univ. Press, New York, 1989).
3. R. A. F. Grieve, *Impact Cratering: Processes and Products*, G. R. Osinski, E. Pierazzo, Eds. (Wiley-Blackwell, Oxford, 2012), pp. 177–193.
4. P. Schulte, L. Alegret, I. Arenillas, J. A. Arz, P. J. Barton, P. R. Bown, T. J. Bralower, G. L. Christeson, P. Claeys, C. S. Cockell, G. S. Collins, A. Deutsch, T. J. Goldin, K. Goto, J. M. Grajales-Nishimura, R. A. F. Grieve, S. P. S. Gulick, K. R. Johnson, W. Kiessling, C. Koeberl, D. A. Kring, K. G. MacLeod, T. Matsui, J. Melosh, A. Montanari, J. V. Morgan, C. R. Neal, D. J. Nichols, R. D. Norris, E. Pierazzo, G. Ravizza, M. Rebolledo-Vieyra, W. Uwe Reimold, E. Robin, T. Salge, R. P. Speijer, A. R. Sweet, J. Urrutia-Fucugauchi, V. Vajda, M. T. Whalen, P. S. Willumsen, The Chicxulub asteroid impact and mass extinction at the Cretaceous–Paleogene boundary. *Science* **327**, 1214–1218 (2010).
5. D. A. Kring, Impact events and their effect on the origin, evolution, and distribution of life. *GSA Today* **10**, 1–7 (2000).
6. G. R. Osinski, L. L. Tornabene, N. R. Banerjee, C. S. Cockell, R. Flemming, M. R. M. Izawa, J. McCutcheon, J. Parnell, L. J. Preston, A. E. Pickersgill, A. Pontefract, H. M. Sapers, G. Southam, Impact-generated hydrothermal systems on Earth and Mars. *Icarus* **224**, 347–363 (2013).
7. D. M. Barringer, Coon mountain and its crater. *Proc. Acad. Nat. Sci. Philadelphia* **57**, 861–886 (1905).
8. B. M. French, N. M. Short, *Shock Metamorphism of Natural Materials* (Mono Book Corp., Baltimore, MD, 1968).
9. R. S. Dietz, Shatter cones in cryptoexplosion structures (meteorite impact?). *J. Geol.* **67**, 496–505 (1959).
10. B. M. French, C. Koeberl, The convincing identification of terrestrial meteorite impact structures: What works, what doesn’t, and why. *Earth Sci. Rev.* **98**, 123–170 (2010).
11. W. Branco, E. Fraas, *Abhandlungen der königlich preussischen Akademie der Wissenschaften*, (Verlag der Königlichen Preussischen Akademie der Wissenschaften, Berlin, 1905), pp. 1–64.
12. R. S. Dietz, *Shock Metamorphism of Natural Materials*, B. M. French, N. M. Short, Eds. (Mono Book Corp., Baltimore, MD, 1968), pp. 267–285.
13. R. S. Dietz, Striated surfaces on meteorites: Shock fractures, not slickensides. *Meteorit. Planet. Sci.* **3**, 31–33 (1966).
14. T. E. Bunch, W. L. Quaide, *Shock Metamorphism of Natural Materials*, B. M. French, N. M. Short, Eds. (Mono Book Corp., Baltimore, MD, 1968), pp. 285–286.

15. D. J. Roddy, L. K. Davis, *Impact and Explosion Cratering*, R. B. Merrill, R. D. J. Pepin, R. O. Pepin, Eds. (Pergamon Press, New York, 1977), pp. 715–750.
16. J.-L. Caty, E. H. Chown, D. W. Roy, A new astrobleme: Ile Rouleau structure, Lake Mistassini, Quebec. *Can. J. Earth Sci.* **13**, 824–831 (1976).
17. M. Higgins, L. Tait, A possible new impact structure near Lac de la Presqu'île, Québec, Canada. *Meteorit. Planet. Sci.* **25**, 235–236 (1990).
18. K. Dewing, B. R. Pratt, T. Hadlari, T. Brent, J. Bédard, R. H. Rainbird, Newly identified “Tununik” impact structure, Prince Albert Peninsula, northwestern Victoria Island, Arctic Canada. *Meteorit. Planet. Sci.* **48**, 211–223 (2013).
19. A. Sagy, Z. Reches, J. Fineberg, Dynamic fracture by large extraterrestrial impacts as the origin of shatter cones. *Nature* **418**, 310–313 (2002).
20. A. Sagy, J. Fineberg, Z. Reches, Shatter cones: Branched, rapid fractures formed by shock impact. *J. Geophys. Res.* **109**, B10209 (2004).
21. G. P. Johnson, R. J. Talbot, *A Theoretical Study of the Shock Wave Origin of Shatter Cones* (Air Force Institute of Technology, Dayton, OH, 1964).
22. P. J. S. Gash, Dynamic mechanism for the formation of shatter cones. *Nature* **230**, 32–35 (1971).
23. D. Baratoux, H. J. Melosh, The formation of shatter cones by shock wave interference during impacting. *Earth Planet. Sci. Lett.* **216**, 43–54 (2003).
24. F. Wieland, W. U. Reimold, R. L. Gibson, New observations on shatter cones in the Vredefort impact structure, South Africa, and evaluation of current hypotheses for shatter cone formation. *Meteorit. Planet. Sci.* **41**, 1737–1759 (2006).
25. B. M. French, *Traces of Catastrophe. Handbook of Shock-Metamorphic Effects in Terrestrial Meteorite Impact Structures* (Lunar and Planetary Institute, Houston, TX, 1998).
26. L. O. Nicolaysen, W. U. Reimold, Vredefort shatter cones revisited. *J. Geophys. Res.* **104**, 4911–4930 (1999).
27. P. B. Robertson, Zones of shock metamorphism at the Charlevoix impact structure, Quebec. *Geol. Soc. Am. Bull.* **86**, 1630–1638 (1975).
28. M. Hasch, W. U. Reimold, P. T. Zaag, U. Raschke, K. Hobson, K. U. Hess, Shatter cones at the Keurusselkä impact structure and their relation to local jointing, 46th Lunar Planetary Science Conference, The Woodlands, Texas, 16 to 20 March, 2015.
29. P. Lambert, The Rochechouart crater: Shock zoning study. *Earth Planet. Sci. Lett.* **35**, 258–268 (1977).
30. H. G. Wilshire, T. W. Offield, K. A. Howard, D. Cummings, *Geology of the Sierra Madera Cryptoexplosion Structure, Pecos County, Texas* (Government Printing Office, Washington, DC, 1972).
31. S. Holm, C. Alwmark, W. Alvarez, B. Schmitz, Shock barometry of the Siljan impact structure, Sweden. *Meteorit. Planet. Sci.* **46**, 1888–1909 (2011).
32. R. M. Stesky, H. C. Halls, Structural analysis of shatter cones from the Slate Islands, northern Lake Superior. *Can. J. Earth Sci.* **20**, 1–18 (1983).
33. J. G. Bray, Shatter cones at Sudbury. *J. Geol.* **74**, 243–245 (1966).
34. G. R. Osinski, P. Lee, J. G. Spray, J. Parnell, D. S. S. Lim, T. E. Bunch, C. S. Cockell, B. Glass, Geological overview and cratering model for the Haughton impact structure, Devon Island, Canadian High Arctic. *Meteorit. Planet. Sci.* **40**, 1759–1776 (2005).
35. E. P. Turtle, E. Pierazzo, G. S. Collins, G. R. Osinski, H. J. Melosh, J. V. Morgan, W. U. Reimold, in *Large meteorite impacts III: Geological Society of America Special Paper 384*, T. Kenkmann, F. Hörz, A. Deutsch, Eds. (Geological Society of America, Boulder, CO, 2005), pp. 1–24.
36. D. E. Gault, J. A. Wedekind, Experimental studies of oblique impact. *Proc. Lunar Planet. Sci. Conf.* **9**, 3843–3875 (1978).
37. G. R. Osinski, J. G. Spray, Tectonics of complex crater formation as revealed by the Haughton impact structure, Devon Island, Canadian High Arctic. *Meteorit. Planet. Sci.* **40**, 1813–1834 (2005).
38. B. C. Johnson, T. J. Bowling, Where have all the craters gone? Earth's bombardment history and the expected terrestrial cratering record. *Geology* **42**, 587–590 (2014).
39. S. Hergarten, T. Kenkmann, The number of impact craters on Earth: Any room for further discoveries? *Earth Planet. Sci. Lett.* **425**, 187–192 (2015).
40. B. A. Hofmann, E. Gnos, New finds of shatter cones in Distal Ries Ejecta, Bernhardtzell, Eastern Switzerland, *Proceedings of 69th Annual Meeting of the Meteoritical Society*, Zurich, Switzerland, 2006.
41. D. J. Milton, A. Y. Glikson, R. Brett, Gosses Bluff—A latest Jurassic impact structure, Central Australia. Part 1: Geological structure, stratigraphy, and origin. *AGSO J. Aust. Geol. Geophys.* **16**, 453–486 (1996).
42. A. P. Crósta, C. Koeberl, R. A. Furuie, C. Kazuo-Vieira, The first description and confirmation of the Vista Alegre impact structure in the Paraná flood basalts of southern Brazil. *Meteorit. Planet. Sci.* **45**, 181–194 (2010).
43. V. L. Sharpton, B. O. Dressler, R. R. Herrick, B. Schnieders, J. Scott, New constraints on the Slate Islands impact structure, Ontario, Canada. *Geology* **24**, 851–854 (1996).
44. P. B. Robertson, La Malbaie structure, Quebec—A palaeozoic meteorite impact site. *Meteoritics* **4**, 89–112 (1968).
45. R. A. F. Grieve, D. Stöffler, A. Deutsch, The Sudbury structure: Controversial or misunderstood? *J. Geophys. Res.* **96**, 22753–22764 (1991).
46. A. Theriault, R. A. F. Grieve, W. U. Reimold, Original size of the Vredefort structure: Implications for the geological evolution of the Witwatersrand Basin. *Meteorit. Planet. Sci.* **32**, 71–77 (1997).
47. D. Stöffler, L. Bischoff, W. Oskierski, B. Wiest, Structural deformation, breccia formation, and shock metamorphism in the basement of complex terrestrial impact craters: Implications for the cratering process, in *Deep Drilling in Crystalline Bedrock*, v. 1, A. Boden, K. G. Eriksson, Eds. (Springer-Verlag, New York, 1988), pp. 277–297.
48. R. Lakomy, Distribution of impact induced phenomena in complex terrestrial impact structures: Implications for transient cavity dimensions. *Proc. Lunar Planet. Sci. Conf.* **21**, 676–677 (1990).
49. T. Kenkmann, M. Poelchau, G. Wulf, Structural geology of impact craters. *J. Struct. Geol.* **62**, 156–182 (2014).
50. J. V. Morgan, M. R. Warner, G. S. Collins, H. J. Melosh, G. L. Christeson, Peak-ring formation in large impact craters: Geophysical constraints from Chicxulub. *Earth Planet. Sci. Lett.* **183**, 347–354 (2000).
51. D. M. H. Baker, J. W. Head, G. S. Collins, R. W. K. Potter, The formation of peak-ring basins: Working hypotheses and path forward in using observations to constrain models of impact-basin formation. *Icarus* **273**, 146–163 (2016).
52. S. W. Kieffer, C. H. Simonds, The role of volatiles and lithology in the impact cratering process. *Rev. Geophys.* **18**, 143–181 (1980).
53. G. R. Osinski, R. A. F. Grieve, G. S. Collins, C. Marion, P. Sylvester, The effect of target lithology on the products of impact melting. *Meteorit. Planet. Sci.* **43**, 1939–1954 (2008).
54. H. J. Melosh, B. A. Ivanov, Impact crater collapse. *Annu. Rev. Earth Planet. Sci.* **27**, 385–415 (1999).
55. G. S. Collins, T. Kenkmann, G. R. Osinski, K. Wünnemann, Mid-sized complex crater formation in mixed crystalline-sedimentary targets: Insight from modeling and observation. *Meteorit. Planet. Sci.* **43**, 1955–1977 (2008).
56. K. Wünnemann, G. S. Collins, G. R. Osinski, Numerical modelling of impact melt production on porous rocks. *Earth Planet. Sci. Lett.* **269**, 529–538 (2008).
57. S. W. Kieffer, P. P. Phakey, J. M. Christie, Shock processes in porous quartzite: Transmission electron microscope observations and theory. *Contrib. Mineral. Petr.* **59**, 41–93 (1976).
58. R. A. F. Grieve, F. Langenhorst, D. Stöffler, Shock metamorphism of quartz in nature and experiment: II. Significance in geoscience. *Meteorit. Planet. Sci.* **31**, 6–35 (1996).
59. H. Dypvik, L. F. Jansa, Sedimentary signatures and processes during marine bolide impacts: A review. *Sediment. Geol.* **161**, 309–337 (2003).
60. M. Schmieder, E. Buchner, Shatter cones in Opalinuston concretions of the Steinheim Basin (SW Germany) Strahlenkegel in Opalinuston-Konkretionen des Steinheimer Beckens (Baden-Württemberg). *Z. Dtsch. Ges. Geowiss.* **164**, 503–513 (2013).
61. H. J. Melosh, Acoustic fluidization: A new geologic process? *J. Geophys. Res.* **84**, 7513–7520 (1979).
62. L. E. Senft, S. T. Stewart, Dynamic fault weakening and the formation of large impact craters. *Earth Planet. Sci. Lett.* **287**, 471–482 (2009).
63. G. S. Collins, H. J. Melosh, B. A. Ivanov, Modeling damage and deformation in impact simulations. *Meteorit. Planet. Sci.* **39**, 217–231 (2004).
64. P. B. Robertson, G. D. Mason, Shatter cones from Haughton Dome, Devon Island, Canada. *Nature* **255**, 393–394 (1975).
65. J. Pohl, D. Stöffler, F. Gall, K. Ernst, in *Impact and Explosion Cratering*, R. B. Merrill, R. D. J. Pepin, R. O. Pepin, Eds. (Pergamon Press, New York, 1977), pp. 343–404.
66. F. C. Taylor, M. R. Dence, A probable meteorite origin for Mistastin Lake, Labrador. *Can. J. Earth Sci.* **6**, 39–45 (1969).
67. H. H. Bostock, *The Clearwater Complex, New Quebec. Geological Survey of Canada Bulletin 178* (Department of Energy, Mines and Resources, Ottawa, 1969).
68. J. Rondot, Impactite of the Charlevoix Structure, Quebec, Canada. *J. Geophys. Res.* **76**, 5414–5423 (1971).
69. M. R. Dence, The nature and significance of terrestrial impact structures, 24th Inter. Geol. Congr. Section **15**, 77–89 (1972).
70. J. Rondot, Charlevoix and Sudbury as gravity-readjusted impact structures. *Meteorit. Planet. Sci.* **35**, 707–712 (2000).
71. R. A. F. Grieve, *Impact Structures in Canada* (Geological Association of Canada, Ottawa, 2006).
72. S. Hietala, J. Moilanen, Keurusselkä—A new impact structure in Central Finland, 35th Lunar Planet. Sci. Conf., 1619 (2004).
73. S. Hietala, J. Moilanen, Keurusselkä—Distribution of shatter cones, 38th Lunar Planet. Sci. Conf., 1762 (2007).
74. L. Ferrière, S. Raïskila, G. R. Osinski, L. J. Pesonen, M. Lehtinen, The Keurusselkä impact structure, Finland—Impact origin confirmed by characterization of planar deformation features in quartz grains. *Meteorit. Planet. Sci.* **45**, 434–446 (2010).
75. L. Ferrière, F. R. T. Lubala, G. R. Osinski, P. K. Kaseti, The newly confirmed Luizi impact structure, Democratic Republic of Congo—Insights into central uplift formation and post-impact erosion. *Geology* **39**, 851–854 (2011).

76. L. Ferrière, P. K. Kaseti, F. R. T. Lubala, J. Akwerali, A. Djuma, New finds of impactites at the Luizi impact structure (Democratic Republic of Congo). *77th Annu. Meet. Meteorit. Soc.* **49**, 5321 (2014).
77. F. Kraut, B. M. French, The Rochechouart meteorite impact structure, France: Preliminary geological results. *J. Geophys. Res.* **76**, 5407–5413 (1971).
78. J. Pohl, K. Ernstson, P. Lambert, Gravity measurements in the Rochechouart impact structure (France). *Meteoritics* **13**, 601–604 (1978).
79. P. Lambert, in *Large Meteorite Impacts and Planetary Evolution IV: Geological Society of America Special Paper 465*, R. L. Gibson, W. U. Reimold, Eds. (Geological Society of America, Boulder, CO, 2010), pp. 509–541.
80. T. J. Goldin, K. Wünnemann, H. J. Melosh, G. S. Collins, Hydrocode modeling of the Sierra Madera impact structure. *Meteorit. Planet. Sci.* **41**, 1947–1958 (2006).
81. R. A. F. Grieve, in *Deep Drilling in Crystalline Bedrock. Volume 1: The Deep Gas Drilling in the Sijjan Impact Structure, Sweden and Astroblemes*, A. Boden, K. G. Eriksson, Eds. (Springer-Verlag, New York, 1988), pp. 328–348.
82. I. von Dalwigk, T. Kenkmann, *Nordic Geological Winter Meeting*, Trondheim, Norway, 1999.

Acknowledgments: We thank R. A. F. Grieve for valuable discussions on this topic; K. Hansen, R. Misener, and A. Singleton for shatter cone data for the Slate Islands impact structure presented in Table 1; J. Newman, C. Marion, and M. Mader for their contributions to field

studies at the Mistastin Lake and Tunnunik impact structures; and T. Bowling, C. Koeberl, and M. Schmieder for their very thorough and constructive reviews. **Funding:** G.R.O. is supported by the Natural Sciences and Engineering Research Council of Canada (NSERC) Industrial Research Chair sponsored by MacDonald Dettwiler and Associates Ltd., the Canadian Space Agency, and the Centre for Excellence in Mining Innovation. We also acknowledge funding from the NSERC Discovery Grant program. Fieldwork at the Haughton and Tunnunik structures was supported by the Polar Continental Shelf Program. **Author contributions:** Both authors contributed extensively to this work. G.R.O. performed the majority of the field investigations, compiled the figures, and conceptualized the paper. L.F. contributed to data interpretations and manuscript at all stages of writing. **Competing interests:** The authors declare that they have no competing interests. **Data and materials availability:** All data needed to evaluate the conclusions in the paper are present in the paper. Additional data related to this paper may be requested from the authors.

Submitted 23 March 2016

Accepted 6 July 2016

Published 5 August 2016

10.1126/sciadv.1600616

Citation: G. R. Osinski, L. Ferrière, Shatter cones: (Mis)understood? *Sci. Adv.* **2**, e1600616 (2016).

Shatter cones: (Mis)understood?

Gordon R. Osinski and Ludovic Ferrière

Sci Adv 2 (8), e1600616.
DOI: 10.1126/sciadv.1600616

ARTICLE TOOLS <http://advances.sciencemag.org/content/2/8/e1600616>

REFERENCES This article cites 59 articles, 8 of which you can access for free
<http://advances.sciencemag.org/content/2/8/e1600616#BIBL>

PERMISSIONS <http://www.sciencemag.org/help/reprints-and-permissions>

Use of this article is subject to the [Terms of Service](#)

Science Advances (ISSN 2375-2548) is published by the American Association for the Advancement of Science, 1200 New York Avenue NW, Washington, DC 20005. 2017 © The Authors, some rights reserved; exclusive licensee American Association for the Advancement of Science. No claim to original U.S. Government Works. The title *Science Advances* is a registered trademark of AAAS.